

## Original Article

MECHANISMS INVOLVED IN THE EXTENSION OF PULMONARY *MYCOBACTERIUM AVIUM* INFECTION FROM THE PULMONARY FOCUS TO THE REGIONAL LYMPH NODES

<sup>1</sup>Kenji HIBIYA, <sup>1</sup>Masao TATEYAMA, <sup>1</sup>Daisuke TASATO, <sup>1</sup>Hideta NAKAMURA,  
<sup>1</sup>Eriko ATSUMI, <sup>1</sup>Futoshi HIGA, <sup>2</sup>Kiyoko TAMAI, and <sup>1</sup>Jiro FUJITA

**Abstract** [Purpose] This study was designed to evaluate the mechanism of *Mycobacterium avium* extension in lung infection. [Study design] Retrospective study. [Participants] A 42-year-old man with acquired immune deficiency syndrome and immune reconstitution inflammatory syndrome. The patient developed mediastinal lymphadenopathy and a peripheral lesion in the right upper lobe within 2 weeks of starting highly active antiretroviral therapy. [Methods] Pulmonary tissue and lymph nodes were dissected under thoracoscopy and evaluated pathologically and immunohistochemically. [Results] Pulmonary pathologic examination revealed extensive granuloma formation throughout the acini. Mycobacterial antigens were found in the macrophages in the alveoli and in the alveolar septa. Some macrophages including mycobacterial antigens were surrounded by lymphatic endothelial cells in the interstitium. In addition, a proliferative granulomatous lesion was found under the intact epithelial layer of a bronchiole. Pathological examination of the lymph nodes revealed aggregated proliferative granulomas with few mycobacteria. Genetically closely related *M. avium* strains were isolated from both tissues. [Conclusions] This study showed the mechanism involved in the progression of pulmonary *M. avium* infection from the pulmonary focus to the regional lymph nodes via the lymphatic vessels.

**Key words:** Extension mechanism, Immune reconstitution inflammatory syndrome, *Mycobacterium avium*

## Introduction

Pulmonary *Mycobacterium avium* complex (MAC) infection begins with nodular lesions in the acini of immunocompetent hosts followed by extensive granuloma formation throughout the airway<sup>1)</sup>. Alternatively, MAC may spread from the alveolar space to the peri-bronchial area through the lymphatic system. In tuberculosis, it has been well established that mycobacteria are transported from the primary focus in the pulmonary parenchyma to the regional lymph nodes via lymphatic vessels<sup>3)4)</sup>. The formation of infectious lesions in regional lymph nodes is rare in MAC infection in immunocompetent patients. In contrast, mediastinal lymphadenopathy is frequently observed in disseminated MAC disease or immune-reconstitution disorders. However, most of these diseases are not complicated by pulmonary parenchymal lesions<sup>5)6)</sup>. In addition, the pathway involved in mycobacterial antigen transmission in pulmonary MAC disease has not been fully documented. We experienced a patient with immune reconstitution resulting from impaired cell-mediated immunity by human

immunodeficiency virus (HIV) infection. This patient showed mediastinal lymphadenopathy with a pulmonary lesion caused by *M. avium* infection. We examined the localization of the mycobacterial antigen in the lung and determined the mechanism involved in the progression of *M. avium* pulmonary infection.

## Materials and Methods

## 1. Clinical presentation

A 42-year-old man suffering from nonproductive cough and shortness of breath was admitted to the hospital. He was diagnosed with *Pneumocystis jirovecii* pneumonia (PJP) and HIV infection. His CD4<sup>+</sup> cell count was 103/ $\mu$ l and his HIV viral load was  $2.4 \times 10^6$  copies/ml. After 3 weeks of treatment for PJP, an improvement was observed in his chest images and laboratory findings. Highly active anti-retroviral therapy (HAART) was started after completing the treatment for PJP. Eight days after starting HAART, the patient developed fever ranging from 38 to 40°C. A chest plain X-ray film revealed lymph node enlargement in the right mediastinal region and a

<sup>1</sup>Department of Infectious, Respiratory, and Digestive Medicine, Control and Prevention of Infectious Diseases, Faculty of Medicine, University of the Ryukyus, <sup>2</sup>Miroku Medical Lab. Inc.

Correspondence to: Kenji Hibiya, Department of Infectious, Respiratory, and Digestive Medicine, Control and Prevention of Infectious Diseases, Faculty of Medicine, University of the Ryukyus, 207 Uehara, Nishihara-cho, Nakagami-gun, Okinawa 903–0215 Japan.  
(E-mail: kenjihibiya@gmail.com)  
(Received 10 Apr. 2010/Accepted 10 Sep. 2010)

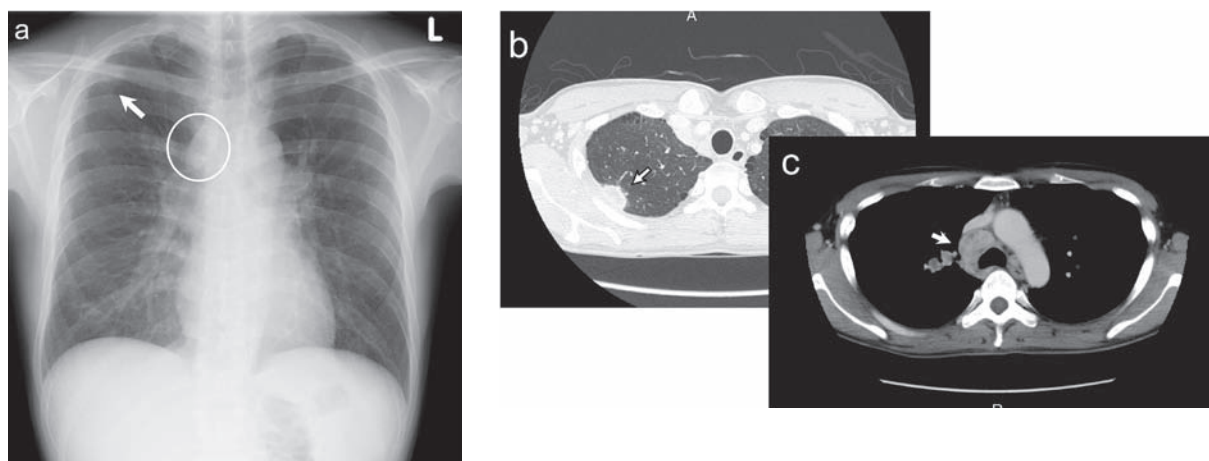


**Fig. 1** Radiologic findings of the pulmonary and mediastinal lesions. a) Chest plain X-ray revealed a coin lesion in the right upper lobe (arrow) and the mediastinal lymphadenopathy (encircled area). b) Chest computed tomography showed a mass (22.5×12.0 mm) attached to the pleura (arrow). c) Chest computed tomography also revealed the mediastinal lymphadenopathy with central low density area (29.5×23.0 mm) (arrow).

coin lesion in the right upper lobe (Fig. 1a). The lymph nodes subsequently enlarged gradually. About one and a half months after starting HAART, a tumor shadow attached to the pleura of the right upper lobe and enlarged lymph nodes with a central low density area were confirmed by chest computed tomography performed before thoracoscopic surgery (Fig. 1b, c). For diagnosis of the lesions, part of the mediastinal lymph nodes and the affected pulmonary segment were excised under thoracoscopic surgery. The pulmonary lesions yielded ashen serous pus that contained numerous granulated acid-fast bacilli with lower acid fastness. Mycobacteria were subsequently cultured from the pus samples and belatedly from the lymph node tissue. The blood culture was negative for these mycobacteria. The organism was identified as *M. avium* by polymerase chain reaction analysis. The patient was discharged several weeks after the surgery showing improvements to anti-mycobacterial medication and HAART.

## 2. Histological analysis

### (1) General histological observation

All specimens were fixed in 10% neutral-buffered formalin and embedded in paraffin. Four- $\mu$ m-thick consecutive tissue sections were prepared from each specimen and fixed to silane-treated glass slides. These sections were then deparaffinized, dehydration, and stained with hematoxylin–eosin (H&E) for general observation and with Victoria blue van Gieson (VVG) to evaluate the fibrotic response. To evaluate reticular fibers in the granulomatous lesion, the tissues were also stained using the silver impregnation method, according to the technique reported by Watanabe & Semprini (1985)<sup>7)</sup>. We then classified the histologic characteristics in terms of exudative reaction/granuloma and proliferative reaction/granuloma based on established criteria<sup>8)</sup>. Briefly, an exudative lesion consists of an

amorphous exudate of mononuclear cells and lymphocytes, and usually extensive necrotic debris. Proliferative reactions are characterized by granulomas composed of aggregated epithelioid cells, lymphocytes, and some Langhans giant cells with variable degrees of central necrosis.

### (2) Immunohistochemical assay

The serial sections were also processed for immunohistochemical assay. Antigen retrieval was performed in a plastic jar filled with target retrieval solution (10 mmol/L citrate buffer, pH 6.0; DakoCytomation, CA, USA) by electric kitchen pot heating at 98°C for 40 min. The appropriate horseradish peroxidase method was performed with the VECTASTAIN ABC-Elite Kit (Vector Laboratories, Burlingame, CA, USA) according to the manufacturer's instructions. The various primary antibodies used for evaluation of the localization of mycobacterial antigen and for exclusive diagnosis in the affected tissues (Table). We confirmed the cross reactivity of an antibody against *Mycobacterium tuberculosis* to MAC in a preliminary study, which has been reported to cross-react with MAC.

Those reacted tissues were followed by revelation with the Vector Impress and DAB kits (Vector Laboratories, Burlingame, CA, USA). In order to test for multiple antigen labeling, Alexa Fluor® 555 (red fluorescence) (Invitrogen, Carlsbad, CA, USA) was used as secondary antibodies, followed by mounting with the VECTASHIELD Mounting Medium with 4', 6 diamidino-2-phenylindole (DAPI) (Vector Laboratories, Burlingame, CA, USA). Nucleus of each tissue sections stained with DAPI showed blue fluorescence. Bright field images were acquired using the Leica DM 1000 LED microscope and DFC 290 camera system (Leica Microsystem, Buckinghamshire, UK), and fluorescent images were obtained using the Olympus BX51 microscope system (Olympus, Shinjuku, Tokyo, JP). All

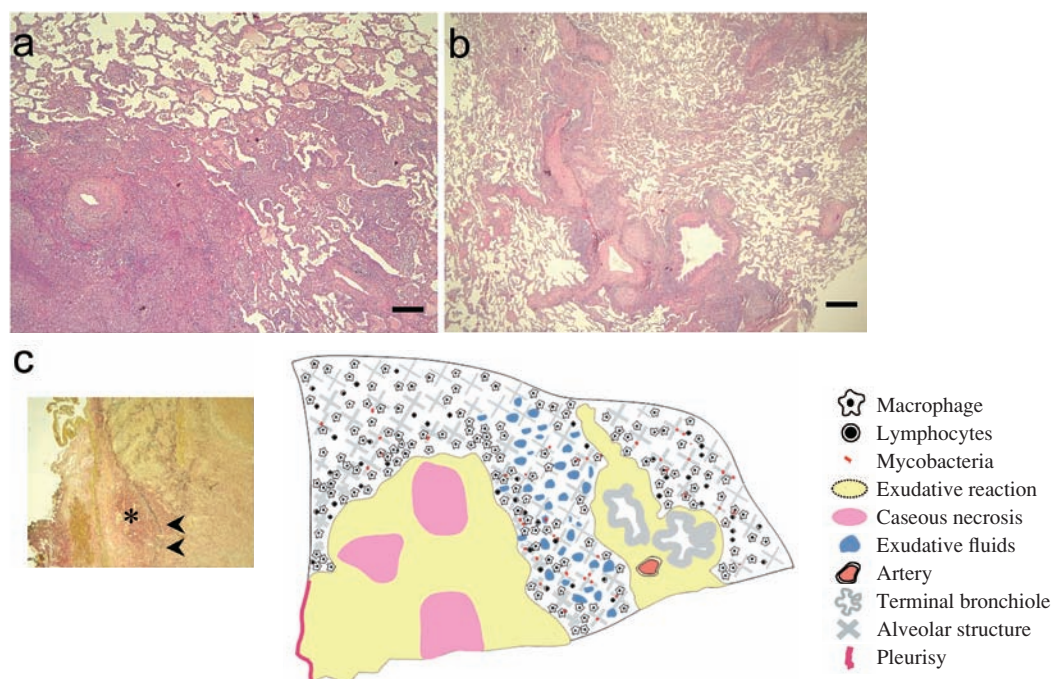


**Fig. 2** Histologic features of the pulmonary lesion. a) Exudative lesions have spread into the surrounding alveoli. Each alveolus is filled with macrophages and inflammatory cells. b) A granulomatous lesion has developed in the sub-epithelial layer of the bronchiole. H&E stain; scale bars, 500  $\mu$ m in “a” and “b”. c) Illustration of the pathological findings of the mass in the peripheral lung. The center of the lesion shows multiple ovoid regions of caseous necrosis. The infiltration of numerous macrophages with some lymphocytes in alveoli was found. The mycobacteria are mainly located in the alveolar septa and within the alveoli with exudative lesions. Granuloma formation around the terminal bronchiole is also evident. c-i) The histological features of the pleuritis with accumulation of collagenous fibrous tissue in the deep connective tissue layer (asterisk) result in thickening of visceral pleura. Arrow heads indicate inner elastic layer. Victoria blue van Gieson stain  $\times 25$ .

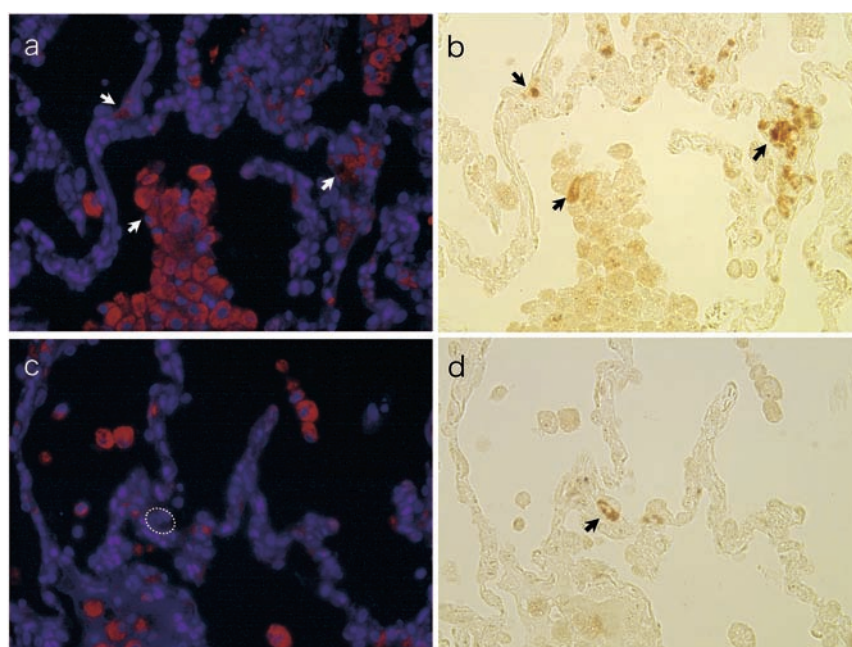


**Fig. 3** Localization of the mycobacterial antigen in the pulmonary lesion. a) Cells stained with the CD 68 antibody are present in the alveolus. CD 68<sup>+</sup> cells (red stain) have accumulated in alveoli and the alveolar septa. b) Mycobacterial antigen (brownish granulated matter) is present in the cytoplasm of CD 68<sup>+</sup> cells, as indicated in “a” (arrows). Most of the cells in the alveolar septa show intense staining for the mycobacterial antigen. c) Negative staining for the CD 68 antibody in the alveolar epithelium (circles/dotted-line). d) Mycobacterial antigen (brown granulated matter) is present in the cytoplasm of CD 68<sup>-</sup> cells, as indicated in “c” (arrow), representing alveolar type II epithelial cells. Original magnification,  $\times 400$  in “a”–“d”.



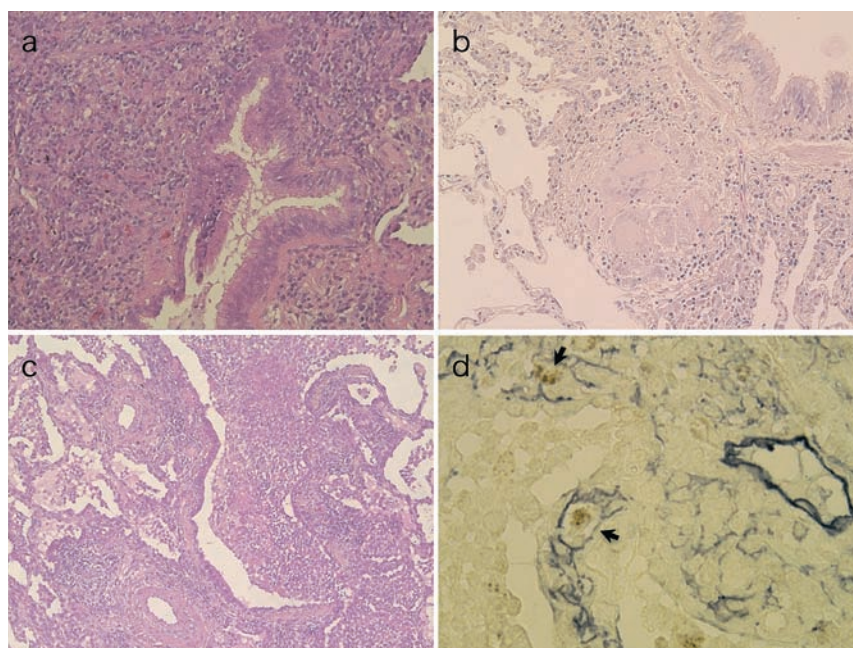


**Fig. 4** Histologic findings indicate the mechanisms involved in the transmission of pulmonary mycobacterial infection. a) Proliferative reaction around the terminal bronchiole. Note the intact epithelium and sub-epithelial granuloma formations. b) Loosely formed proliferative granuloma in the sub-epithelial layer of the terminal bronchiole. c) Narrowing of the bronchiolar air space caused by a granulomatous exudate protruding into the bronchial lumen. Note cellular exudates inside the respiratory bronchiole. d) Immunohistochemical staining with the D2-40 monoclonal antibody. Lymphatic vessels are surrounded by D2-40<sup>+</sup> cells. Note the mycobacterial antigen inside the lymphatic vessel (brownish granulated matter, arrow). H&E stain in “a”–“c”; original magnification,  $\times 100$  in “c”,  $\times 200$  in “a” and “b”,  $\times 400$  in “d”.

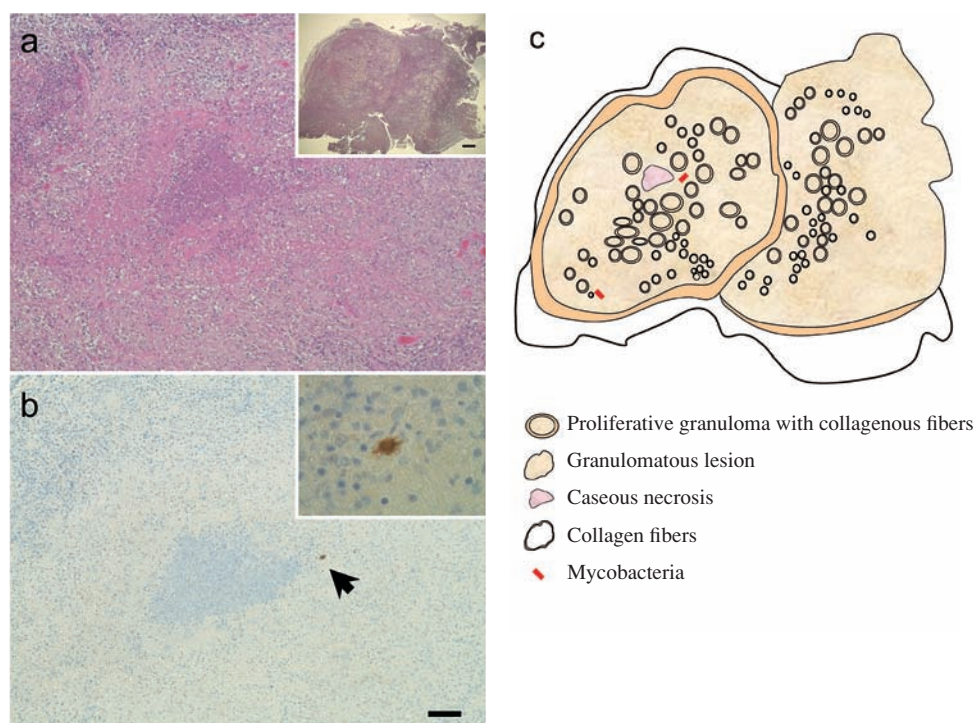


**Fig. 5** Histological features of the granulomatous lesion in the mediastinal lymph node. a) Nonspecific inflammatory reaction around the caseous necrosis (a) and entire picture of the lymph node (a-inset). b) Localization of the mycobacteria in the granulomatous lesion. The arrow indicates a cell containing aggregates stained for mycobacterial antigen (b-inset). c) Illustration of the granulomatous lesion in the mediastinal lymph node. The individual proliferative granulomas have aggregated and formed a single large granuloma. Original magnification,  $\times 200$  (a),  $\times 25$  (a-inset),  $\times 200$  (b),  $\times 1,000$  (b-inset). H & E stain (a), Silver impregnation staining (a-inset), Immunohistochemical staining for Mycobacterial antigen (b, b-inset).

**Table** Antibodies used in this study

Antibody	Clone	Clonality	Specificity	Dilution rate	Source
CD68	514H12	Monoclonal	Monocytes lineage cells	1: 80	Novocastra Laboratories, Newcastle, Tyne and Wear, UK
D2-40	D2-40	Monoclonal	Lymphatic endothelium	1: 50	DakoCytomation, Carpinteria, CA, USA
<i>Pneumocystis carinii</i>	3F6	Monoclonal	<i>Pneumocystis jirovecii</i>	1: 200	Santa Cruz Biotechnology, Santa Cruz, CA, USA
Cytomegalovirus (pp65 antigen)	2 and 6	Monoclonal	Cytomegalovirus pp 65 antigen	1: 200	Novocastra Laboratories, Newcastle, Tyne and Wear, UK
Human herpesvirus (type 8)	13B10	Monoclonal	HHV-8 latent nuclear antigen-1 (LNA-1)	1: 50	Novocastra Laboratories, Newcastle, Tyne and Wear, UK
HIV p24	Kal-1	Monoclonal	HIV p24	1: 25	Vector Laboratories, Burlingame, CA, USA
<i>Mycobacterium tuberculosis</i>	1.1/3/1	Monoclonal	Mycobacterial species	1: 80	Vector Laboratories, Burlingame, CA, USA

HIV: human immunodeficiency virus; HHV: human herpes virus.

sections were evaluated independently by two pathologists (KH and EA).

### 3. Genotypic analysis

The DNA fragment patterns of *M. avium* strains isolated from pulmonary lesion and mediastinal lymph node were analyzed by Pulse-field gel electrophoresis (PFGE) as described previously<sup>9)</sup>. Isolates cultured purely from a single colony from third isolation plate. Reference isolate were used no.3 (isolate obtained from a disseminated case), no.4 (pig isolate), no.5 (ATCC 25291). Gel electrophoresis performed with condition that 19.7 hours, 6.0V/cm, 120° angles with *Xba* I (TOYOBO, Osaka-shi, Osaka, JP) restriction enzyme. PFGE genotypic pattern was analyzed by Fingerprinting II Software Ver. 3.0. Interpretation of the analysis results was defined as follows: indistinguishable, when the genotypic pattern have the same numbers of bands with the same apparent size; identical, when the genotypic pattern differed by only 1–3 bands; and unrelated, when the genotypic pattern differed by 4 or more bands<sup>9)10)</sup>.

## Results

### 1. Histologic findings of the pulmonary lesion

The pulmonary lesion showed exudative reactions inside the alveoli (Fig. 2a). The alveolar spaces around regions of caseous necrosis showed accumulation of macrophages. Granulomatous lesions were also formed in the peri-bronchiolar areas (Fig. 2b). Interestingly, the mycobacterial antigens were mainly distributed in the periphery of the granulomatous lesions (Fig. 2c).

The CD 68<sup>+</sup> cells containing mycobacterial antigens were located in the septa of the alveoli around the granulomatous lesion (Fig. 3a, b). Many CD 68<sup>+</sup> cells were also aggregated in the alveoli (Fig. 3a), but mycobacterial antigens were detected inside the some CD 68<sup>+</sup> cells (Fig. 3b). The intensity of mycobacterial antigens was higher in the CD 68<sup>+</sup> cells in the septa than in the CD68<sup>+</sup> cells inside the alveolus (Fig. 3b). Alveolar type II epithelial cells were negative for CD 68

monoclonal antibody (Fig. 3c). The cytosol of a few CD 68<sup>+</sup> cells, representing alveolar type II cells, were positively stained for mycobacterial antigen (Fig. 3c, d).

### 2. Histological findings of the peri-bronchial lesion

A proliferative reaction composed of epithelioid cells and lymphocytes was observed in the peri-bronchiolar area (Fig. 4a). The membranous bronchiole had an intact epithelial layer. Proliferative granulomas with some Langhans multinucleated giant cells were present in the submucosal area of the terminal bronchiole (Fig. 4b). Proliferation of the granulomas also caused destruction of the muscularis mucosa. In some areas of the exudative lesions, the protrusion of exudates from the peri-bronchial granuloma into the lumen of the respiratory bronchiole was observed, resulting in marked narrowing of the bronchiole (Fig. 4c). D2-40<sup>+</sup> cells were prominently distributed in the granulomatous lesion. Importantly, D2-40<sup>+</sup> cells surrounded the cells containing the mycobacterial antigen (Fig. 4d).

### 3. Histological findings of the pleural lesion

The accumulation of collagenous fibrous tissue between the visceral pleura and the granulomatous lesion was also found (Fig. 2c-inset). Mild lymphocytes infiltration was also observed in the visceral pleura. However, granulomatous lesions and caseation necrosis were not observed in the pleura.

### 4. Histological findings of the lymph node lesion

The dissected mediastinal lymph node principally contained aggregated proliferative granuloma composed of epithelioid cells and lymphocytes (Fig. 5a). Several granulomatous structures were encapsulated with collagenous fibers. In addition, the silver impregnation stain revealed the formation of reticular fibers within the granulomas (not shown). Comparatively minor caseous necrosis was observed in some serial sections of the lymph node. There were very few neutrophils inside or around the regions of caseous necrosis, which were surrounded by granulation tissue (Fig. 5a). Mycobacterial antigens were

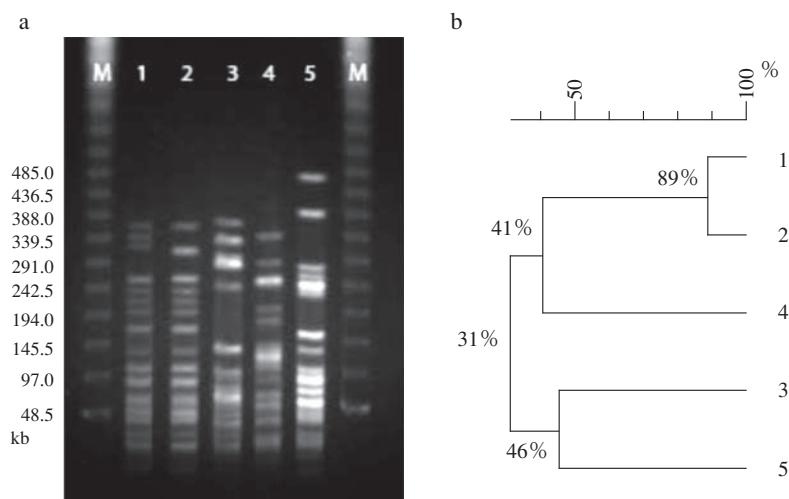


**Fig. 6** PFGE pattern of isolates from pulmonary lesion and mediastinal lymph node (a) and schematic diagram showing the differences (b). M: molecular marker. 1: *M. avium* isolated from the pulmonary lesion, 2: *M. avium* isolated from the mediastinal lymph node, 3: *M. avium* isolated from mesenteric lymph node in a pig, 4: *M. avium* obtained from a disseminated case associated with HIV infection, 5: standard strain of *M. avium* (ATCC 25291).

only observed in the cytosol of a few epithelioid cells located in the peripheral region of the caseous necrosis (Fig. 5b, c).

#### 5. The result of pulse-field gel electrophoresis

Mycobacteria isolated from pulmonary lesion showed the defect of one band compared with the isolate from mediastinal lymph nodes (Fig. 6a, no.1/no.2), which the affinity of the both PFGE pattern was 89% (Fig. 6b).

### Discussion

The present study demonstrated the mechanisms by which an MAC infectious lesion extended from the pulmonary parenchymal lesion to the regional lymph nodes through lymphatic vessels and its infectiveness into alveolar macrophages and type II alveolar epithelial cells.

In general, a pulmonary MAC infection in an immunocompetent host merely shows acinar nodular lesions or peri-bronchiolar granulomas<sup>8)</sup>. As the mechanisms involved in the development of pulmonary MAC infectious lesions, the acinar extension pattern, the bronchial extension pattern and the lymphatic extension pattern were previously proposed<sup>11)</sup>. In this study, the granulomatous lesion with caseous necrosis extended through the pulmonary acini. In addition, infiltration of peripheral mononuclear cells into the alveoli was observed. This histologic finding is common in the initial stage of tuberculosis<sup>12)</sup> and is known as granulomatous pneumonia<sup>8)13)</sup>. Similar findings were also reported in MAC disease<sup>1)14)</sup>.

In this study, most of the infected cells were monocyte-lineage cells in the alveoli and in the alveolar septa around the granulomatous lesion. This observation suggests that macrophages phagocytose mycobacteria in the alveoli and then translocate into the alveolar septa<sup>15)</sup>. In addition, the finding

that mycobacterial antigens were found in the cytoplasm of alveolar type II epithelial cells is consistent with the results of studies that examined the ability of *M. avium* to adhere to alveolar epithelial cells and to invade alveolar epithelial cells *in vitro*<sup>16)17)</sup>. However, mycobacterial antigens were present in the cytoplasm of a small number of alveolar type II epithelial cells. Therefore, we suggest that alveolar type II epithelial cells have little impact on the progression of the MAC infection. However, our results do not exclude the involvement of alveolar type II epithelial cells for the induction of the initial immune response through the production of chemokines or cytokines<sup>18)~20)</sup>.

In the present case, the proliferative granulomas were formed in the submucosal area of the terminal bronchiole with an intact epithelial layer, as reported by some researchers<sup>1)14)</sup>. An *in vitro* study on the mechanism involved in the extension of *M. avium* to the peri-bronchial area showed that the mycobacteria invade the polarized monolayers of BEAS-2B bronchial cells, and then translocate to the opposite side across the monolayers<sup>2)</sup>. However, we could not detect any mycobacterial antigens in the bronchiolar epithelial cells or in the submucosal area. In contrast, macrophages containing mycobacterial antigens were located in lymphatic vessels. This finding suggests that organism spreads from the alveolar space to the lymphatic vessels along bronchiole. To our knowledge, although this mechanism of progression has been described in tuberculosis<sup>21)</sup>, this is the first report in pulmonary MAC infection.

In this study, the pleuritis was caused by contiguous invasion from a subpleural focus, but the histology showed the diffuse infiltration of lymphoid cells without a granulomatous reaction and without organism. Kakugawa et al. (2008) previously reported that *M. avium* pleuritis with pleural effusion in a non-



compromised patient showed non-specific inflammation<sup>22</sup>). Based on these findings, we suggest that the sub-pleural granulomatous lesion developed as a host reaction.

In the present case, mediastinal lymphadenopathy was observed with the appearance of a pulmonary lesion, and the existence of genetically closely identical *M. avium* was demonstrated in both pulmonary lesion and lymphoid tissue. In addition, macrophages containing mycobacterial antigen were located in lymphatic vessels. These results indicate that the granulomatous lesions in the lymph nodes were formed by transport of mycobacterial antigens to the mediastinal lymph nodes through the lymphatic vessels. In non-tuberculous mycobacterial infection, pulmonary lesions accompanied by lymphadenopathy are relatively rare<sup>9) 23)</sup>. We are possibly exposed to polyclonal infections of MAC from our environment<sup>24)</sup>. Consequently, with repeated exposure, we may have established significant and specific immunity to MAC<sup>25)</sup>. Kawabata has reported that alveolar macrophages phagocytized the mycobacterial antigen might be mobile, as the result the macrophages could enter the regional lymph nodes within the primary mycobacterial infection, and meanwhile, the macrophages are immobilized by the production of the proliferative granulomas in hosts with acquired immunity, and the macrophages are thus unable to translocate to the regional lymph nodes<sup>26)</sup>. Therefore, we considered that the formation of the lymph node lesion with pulmonary focus similar to the primary complex caused by tuberculosis<sup>3)</sup> is conceivable pathogenesis in pulmonary MAC infection under the IRIS with HIV infection although it is unknown whether the infection is primary or secondary in this case. Further studies are needed to examine the histological characteristics of regional lymph nodes to determine the mechanism involved in the progression of pulmonary MAC infection in immunocompetent hosts.

In this study, hyperplasia of alveolar type II epithelial cells was observed in the perifocal inflammatory areas of the granulomatous lesions. It has been reported that the proliferation of alveolar type II epithelial cells is caused by the repair of damaged alveolar epithelium as a result of pneumonia or a non-specific etiology<sup>20)</sup>. Von Huebschmann has reported the presence of hyperplasia in the initial stage of pulmonary tuberculosis<sup>27)</sup>. Therefore, the host reaction for pulmonary MAC infection may be similar to that of tuberculosis.

In summary, our study has demonstrated the mechanism involved in the progression of pulmonary *M. avium* infection. However, we should be careful to apply this conclusion to pulmonary MAC diseases in immunocompetent patients because these findings were caused under the special condition that the host was during the immune-reconstitution condition with HIV infection.

#### Acknowledgments

The authors are grateful to all those involved in this study, particularly the assistance provided by staff in the Department

of Internal Medicine, the Department of Surgery, and the Clinical Laboratories at University Hospital, University of the Ryukyus.

#### References

- 1) Fujita J, Ohtsuki Y, Suemitsu I, et al.: Pathological and radiological changes in resected lung specimens in *Mycobacterium avium intracellulare* complex disease. *Eur Respir J*. 1999 ; 13 : 535–540.
- 2) Yamazaki Y, Danelishvili L, Wu M, et al.: The ability to form biofilm influences *Mycobacterium avium* invasion and translocation of bronchial epithelial cells. *Cell Microbiol*. 2006 ; 8 : 806–814.
- 3) Ranke KE: Primaeraffekt, sekundaere und tertiaere Stadien d, Lungentbk auf Grund von histologischen Untersuchungen der Lymphdruesen der Lungenpforte. *Deutsch Arch f Klin Med*. 1916 ; 119 : 201–297.
- 4) Shimao T: Tuberculosis primary infection. *Kekkaku*. 2009 ; 84 : 499–502.
- 5) Hocqueloux L, Lesprit P, Herrmann JL, et al.: Pulmonary *Mycobacterium avium* complex disease without dissemination in HIV-infected patients. *Chest*. 1998 ; 113 : 542–548.
- 6) Lawn SD, Bekker LG, Miller RF: Immune reconstitution disease associated with mycobacterial infections in HIV-infected individuals receiving antiretrovirals. *Lancet Infect Dis*. 2005 ; 5 : 361–373.
- 7) Watanabe I, Semprini M: Light and electron microscopy observation in the rat gingival nerve endings. A silver impregnation and a transmission electron microscopy study. *Rev Bras Ciênc Morfol*. 1985 ; 2 : 10–18.
- 8) Tomashefski JF, Farver CF: Tuberculosis and nontuberculous Mycobacterial infections. Dail and Hammar's pulmonary pathology. Volume I. Nonneoplastic lung disease. Tomashefski JF et al. ed., Third ed., Springer, New York, 2008, 316–348.
- 9) Tenover FC, Arbeit RD, Goering RV, et al.: Interpreting chromosomal DNA restriction patterns produced by pulsed-field gel electrophoresis: criteria for bacterial strain typing. *J Clin Microbiol*. 1995 ; 33 : 2233–2239.
- 10) Nishiuchi Y, Tamura A, Kitada S, et al.: *Mycobacterium avium* complex organisms predominantly colonize in the bathtub inlets of patients' bathrooms. *Jpn J Infect Dis*. 2009 ; 62 : 182–186.
- 11) Kawamoto H: A computed tomography-based study of futures development patterns: *Mycobacterium avium* complex without predisposing conditions. *Nihon Kokyuki Gakkai Zasshi*. 1998 ; 36 : 928–933.
- 12) Iwasaki T: The pathology of tuberculosis (in Japanese), JATA books No.3, Japan Anti-Tuberculosis Association, Tokyo, 1997.
- 13) Ogata H: The chest CT findings and pathologic findings of pulmonary tuberculosis. *Kekkaku*. 2009 ; 84 : 559–568.
- 14) Hebisawa A, Tsuchiya K, Tamura A: Pulmonary *Mycobacterium avium* complex disease (in Japanese). *Byouri to rinsho*

- (Pathol Clin Med). 2005 ; 23 : 501–508.
- 15) Danelishvili L, Bermudez LE: Role of type I cytokines in host defense against *Mycobacterium avium* infection. Curr Pharm Des. 2003 ; 9 : 61–65.
  - 16) Bermudez LE, Goodman J: *Mycobacterium tuberculosis* invades and replicates within type II alveolar cells. Infect Immun. 1996 ; 64 : 1400–1406.
  - 17) Sato K, Ogasawara K, Akaki T, et al: Internalization and replication of *Mycobacterium tuberculosis* and *M. avium* complex within type II alveolar epithelial cell line. Kekkaku. 1999 ; 74 : 655–660.
  - 18) Sangari FJ, Petrofsky M, Bermudez LE: *Mycobacterium avium* infection of epithelial cells results in inhibition or delay in the release of interleukin-8 and RANTES. Infect Immun. 1999 ; 67 : 5069–5075.
  - 19) Rao SP, Hayashi T, Catanzaro A: Release of monocyte chemoattractant protein (MCP)-1 by a human alveolar epithelial cell line in response to *Mycobacterium avium*. FEMS Immunol Med Microbiol. 2000 ; 29 : 1–7.
  - 20) Masson RJ: Biology of alveolar type II cells. Respirology. 2006 ; 11 Suppl. : S12–S15.
  - 21) Basaraba RJ, Smith EE, Shanley CA, et al.: Pulmonary lymphatics are primary sites of *Mycobacterium tuberculosis* infection in guinea pigs infected by aerosol. Infect Immun. 2006 ; 74 : 5397–5401.
  - 22) Kakugawa T, Mukae H, Kajiki S, et al.: *Mycobacterium avium* pleuritis in a non-immunocompromised patients. Intern Med. 2008 ; 47 : 1727–1731.
  - 23) Marchevsky A, Damsker B, Gribetz A, et al.: The spectrum of pathology of nontuberculous mycobacterial infections in open-lung biopsy specimens. Am J Clin Pathol. 1982 ; 78 : 695–700.
  - 24) Kuwabara K, Watanabe Y, Wada K, et al.: Molecular epidemiological analysis by IS1245 based restriction fragment length polymorphism typing on cases with pulmonary *Mycobacterium avium* disease observed in the same family. Kekkaku. 2004 ; 79 : 519–523.
  - 25) Kitada S, Maekura R, Toyoshima N, et al.: Use of glycopeptidolipid core antigen for serodiagnosis of *Mycobacterium avium* complex pulmonary disease in immunocompetent patients. Clin Diagn Lab Immunol. 2005 ; 12 : 44–51.
  - 26) Kawabata Y: Pathogenesis of tuberculosis. Nippon Rinsho. 1998 ; 56 : 3041–3046.
  - 27) von Huebschmann P: Pathologische anatomie der Tuberkulose. Julius Springer, Berlin, 1928.